A NEW CLASSIFICATION OF THE AMINO ACID SIDE CHAINS BASED ON DOUBLET ACCEPTOR ENERGY LEVELS

SCOTT F. SNEDDON,* RICHARD S. MORGAN,‡ AND CHARLES L. BROOKS III*
*Department of Chemistry, Carnegie-Mellon University, Pittsburgh, Pennsylvania 15213; and
‡Department of Molecular and Cell Biology, Pennsylvania State University, University Park, Pennsylvania 16814

ABSTRACT We describe a new classification of the amino acid side chains based on the potential energy level at which each will accept an extra (doublet) electron. The doublet acceptor energy level, and the doublet acceptor orbital were calculated using semiempirical INDO/2-UHF molecular orbital theory. The results of these calculations show that the side chains fall into four groups. We have termed these groups repulsive, insulating, semiconducting, and attractive in accordance with where each lies on the relative energy scale. We use this classification to examine the role of residues between the donor and acceptor in modulating the rate and mechanism of electron transfer in proteins. With the calculated acceptor levels, we construct a potential barrier for those residues between the donor and acceptor. It is the area beneath this barrier that determines the decay of electronic coupling between donor and acceptor, and thus the transfer rate. We have used this schematic approach to characterize the four electron transfer pathways in myoglobin recently studied by Mayo et al. (Mayo, S. L., W. R. Ellis, R. J. Crutchley, and H. B. Gray. 1986. *Science* [*Wash. DC*]. 233:948–952).

INTRODUCTION

Several schemes exist for the classificatoin of the amino acid side chains (1, 2). These classifications, in general, reflect an ordering of the side chains with respect to certain measurable properties. Hydrophobicity scales, for example, reflect differences between side chain interactions in polar and apolar solvents. Hydrophobicity has been used to predict which side chains are likely to be folded within the protein, and which are likely to be on the surface (3–5). Hydrophobicity arguments have also been used to rationalize binding and aggregation properties of proteins. A scale of pK values for the ionizable side chains as determined by nuclear magnetic resonance (6) and calculation (7) gives clues to the charged state of the protein as a function of pH. Shifts in pK provide information about the local environment of ionizable residues. These classification schemes allow one to predict how certain side chains will effect a given physical property such as titration behavior or protein folding.

Detailed in this paper is a new classification of the amino acid side chains based on the potential energy level at which an extra (doublet) electron will be accepted. This energy level is termed the doublet acceptor level. We have calculated the doublet acceptor energy, and doublet acceptor orbital, the molecular orbital corresponding to the doublet acceptor energy level, using semiempirical INDO/2-UHF molecular orbital theory (8, 9). From the results of these calculations we find that the side chains fall into four groups which we have termed repulsive, insulating, semiconducting, and attractive. This classification ranks the side chains in their increasing ability to accept an extra electron. We are currently applying this classification to examine the role of the residues which lie between the donor and acceptor in modulating the rate and mechanism of electron transfer in proteins.

Marcus theory offers classical description of the dependence of charge transfer kinetics on donor and acceptor energy levels and spatial separation (10). This theory has been widely applied (10) and has proven quite successful in correlating electron transfer rates with a small number of measurable properties over a wide range of systems; for example, Marcus theory has been applied to electron transfer at electrodes and between biological molecules in solution. In Marcus theory, solvent, or environmental fluctuations create a local electric field which brings into coincidence electronic energy levels of the donor and acceptor. At this transition point, the electron may transfer by barrier-tunneling, with the transmission coefficient being proportional to the electronic coupling between donor and acceptor. Within this theory the rate then depends on the free energy required to attain the nuclear configuration of the transition point, and on the height and

This paper is dedicated to the memory of Albert Szent-Gyorgyi (1893–1986)

shape of the tunneling barrier. The current study provides insight into the latter.

The remainder of this paper is divided into three sections. In the first section we describe the details of the calculations. In the second section we present the results of these calculations. We show the ranking of the side chains in this classification, and describe the orbitals involved in accepting the extra electron. The final section provides a discussion of the classification scheme and a first application to the estimation of medium effects on electron transfer in biological molecules. The focus of this application is on the four pathways in the ruthenium-modified myoglobin model system (11).

METHODS

Details of the Calculation

To calculate the doublet acceptor energy level we employ the INDO program of Zerner and co-workers (12). We have used INDO/2-UHF theory (8, 9) to determine the eigenvalue associated with placing an extra, unpaired (doublet) electron on each of the side chains. This energy level is the sum of attractions and repulsions the electron feels in the highest occupied molecular orbital. According to Koopmans' theorem (13), this eigenvalue ϵ_i^α is related to the negative of the electron ionization potential. The equation for this energy level is

$$\epsilon_i^\alpha = H_{ii}^\alpha + \sum_j^p (J_{ij} - K_{ij}) + \sum_j^q J_{ij}, \qquad (1)$$

where ϵ_i^α is generally called the one electron energy, H_{ii}^α is the average kinetic plus nuclear-electronic attraction energy, J_{ij} is the coulomb integral and K_{ij} is the exchange integral. These latter quantities are given by

$$K_{ij} = \int\int \psi_i(1)\psi_j(2)\frac{1}{r_{12}}\psi_j(1)\psi_i(2)\,d\tau_1 d\tau_2 \qquad (2)$$

$$J_{ij} = \int\int \psi_i(1)\psi_j(2)\frac{1}{r_{12}}\psi_i(1)\psi_j(2)\,d\tau_1 d\tau_2. \qquad (3)$$

The sums in Eq. 1 are over p, the number of alpha electrons, and q, the number of beta electrons (here $p = q + 1$). Details of the approximations made in determining these integrals in the INDO formalism can be found in reference 9. In addition to the standard basis set functions used by Zerner et al. (12), sulfur 3d orbitals were included for the calculation of the methionine, cysteine, and Cys-Cys disulfide acceptor levels.

The nuclear coordinates of the side chains have been taken from the protein crystal structure of myoglobin (14). Each side chain was formed by removing the peptide group, and replacing the C^β-C^α bond with a C^β-H bond. Hydrogen atoms were added to the rest of the side chain based on geometric constraints. Thus the alanine side chain is represented by methane, the phenylalanine side chain by toluene, and so forth. Histidine was calculated in both charged and uncharged forms, as were aspartic acid, and glutamic acid. The peptide group was treated as a separate functional group, and was assigned an acceptor level equal to that of the asparagine side chain. We have assumed that the peptide group represents a small and relatively constant perturbation that should not significantly alter the side chain grouping (15, 16).

The INDO/2-UHF calculation for the charged glutamic acid$^-$ and aspartic acid$^-$ side chains (calculated as glutamic acid^{2-} and aspartic acid^{2-}) predicted that several occupied orbitals were above the dissociation limit. This is not a physically meaningful result, and is attributed to the small basis set used in the INDO approximation. This is supported by the fact that *ab initio* calculations with limited basis sets (STO-3G) give similar results, while calculations with basis sets including diffuse functions (6-31+G) predict only one electron above the ionization limit (Sneddon, S. F., unpublished results). The values given for the doublet acceptor levels of glutamic acid$^-$ and aspartic acid$^-$ are estimates based on the results of these *ab initio* calculations.

We have used the Quantum Chemistry Program Exchange (QCPE) program *PSI/77* (18) to generate an orbital contour plot for representative acceptor orbitals from each of the four groups. The orbital plots show the envelope of the molecular orbital at a contour level of 0.06 atomic units; dashed lines represent a change in sign of the orbital. Orbital plots of the glutamic acid$^-$ and aspartic acid$^-$ acceptor orbitals are not given.

RESULTS

Doublet Acceptor Levels

As shown in Fig. 1, the side chains fall into four groups based on their doublet acceptor level. The negatively charged side chains of glutamic acid$^-$ and aspartic acid$^-$ show the highest energy for the doublet electron. We have called these the repulsive side chains in accord with the unfavorable nature of adding an electron to a negatively charged group. In the next group are the aliphatic and hydroxylic side chains: alanine, leucine, isoleucine, valine, serine, and threonine. This group of side chains accepts an electron at a lower energy than the acids but still at a positive energy, and are thus termed the insulating side chains. The next group, containing the side chains of phenylalanine, tyrosine, histidine, tryptophan, asparagine, glutamine, methionine, cysteine, and the Cys-Cys disulfide, accepts an electron near the zero of energy. Since these side chains accept an extra electron near the binding limit (zero energy), we have called them the semiconducting side chains. The positively charged side chains of lysine$^+$, arginine$^+$, and histidine$^+$ are at negative energy levels. Since the acceptor level for these groups is at a moderately negative value, we have termed them the attractive side chains.

Doublet Acceptor Orbitals

The doublet acceptor orbitals of the repulsive side chains (not shown) are of π^* symmetry and are localized on the

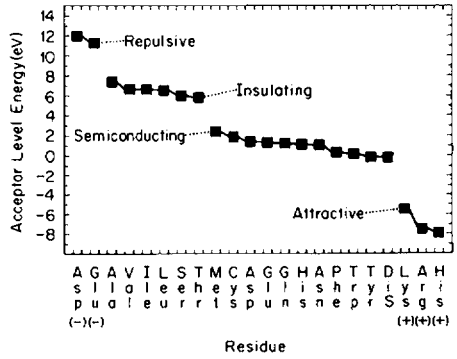

FIGURE 1 Doublet acceptor level groupings for each of the amino acid side chains. The side chains fall into four groups termed repulsive, insulating, semiconducting, and attractive in order of decreasing potential energy.

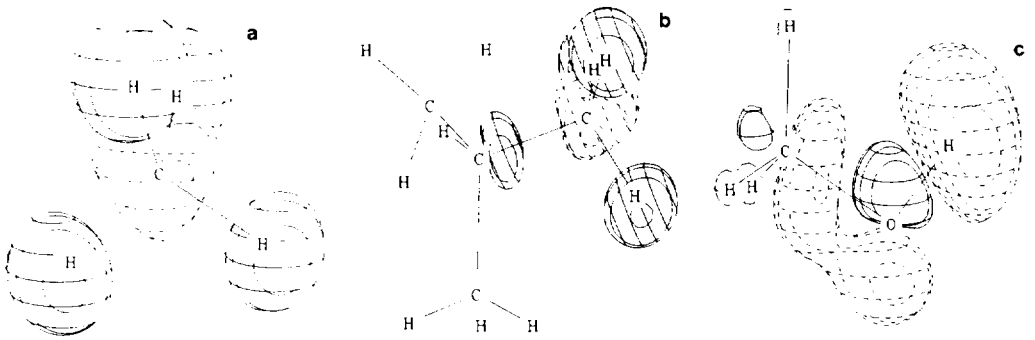

FIGURE 2 Representative doublet acceptor orbitals for the insulating group of side chains: Ala, Val, Ile, Leu, Ser, and Thr. (*a*) The acceptor orbital of the alanine side chain is antibonding between carbon and hydrogens. (*b*) The leucine orbital orbital is similar to alanine, as are the orbitals of isoleucine and valine. (*c*) The acceptor orbital of serine (threonine is similar).

carboxyl group. The orbitals have a slightly larger density on the carbon than on either oxygen.

The acceptor orbital of the insulating side chain alanine is antibonding between the carbon and hydrogens (Fig. 2 *a*). The side chains of leucine (Fig. 2 *b*), isoleucine, and valine have acceptor orbitals similar to alanine. This orbital is localized on C^{γ} in valine and on C^{δ} in leucine and isoleucine, respectively. The acceptor orbitals of serine and threonine have large electron density on the hydroxyl group (Fig. 2 *c*).

The acceptor orbital of the semiconducting side chains methionine and cysteine are predominately $3dx^2 - y^2$ in character (Fig. 3 *a*). In both cases the orbital is bonding between the sulfur and the atoms connected to it. The Cys-Cys disulfide orbital, also of d symmetry, is antibonding between the sulfur atoms, and projects away from each sulfur along the line joining them (Fig. 3 *b*). The acceptor orbitals of each of the ring-containing side chains have π^* symmetry. Within our model, the phenylalanine orbital is identical to a benzene π^* orbital. It is antibonding between $C^{\delta 1}$ and $C^{\epsilon 1}$, and between $C^{\delta 2}$ and $C^{\epsilon 2}$. The tyrosine orbital is the same and is antibonding between the identical pairs of atoms (Fig. 3 *c*). The tryptophan acceptor orbital extends over the entire ring with little electron density at $N^{\epsilon 1}$ (Fig. 3 *d*). The orbital of histidine also extends across the ring. The amide side chains asparagine and glutamine both have

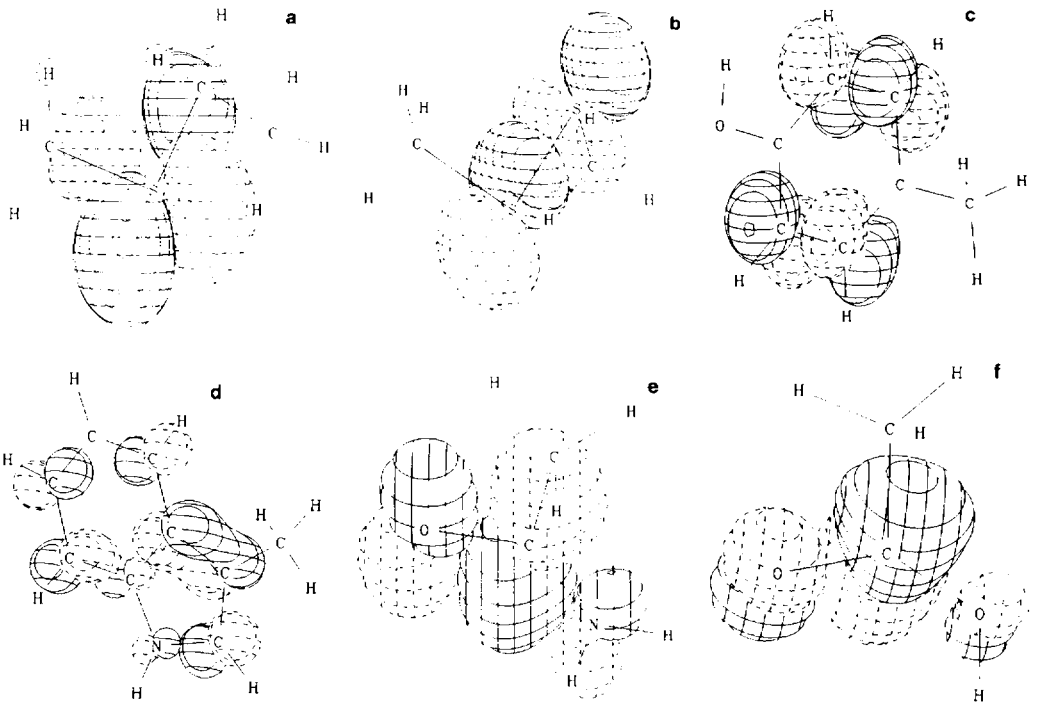

FIGURE 3 Representative doublet acceptor orbitals for the semiconducting group of side chains: Met, Cys, Asp, Glu, Gln, His, Asn, Phe, Trp, Tyr, and Cys-Cys disulfide. (*a*) Methionine, showing the 3d character of the acceptor orbital (Cys is similar). (*b*) Cys-Cys disulfide, 3d in character, antibonding between the sulfurs. (*c*) Tyrosine orbital (Phe is similar). (*d*) Tryptophan. (*e*) Asparagine orbital (glutamine is similar). (*f*) Protonated aspartic acid orbital (protonated glutamic acid is similar).

classic amide π^* orbitals (19) (Fig. 3 *e*). The protonated acids have similar π^* orbitals delocalized over the carbon and both oxygens (Fig. 3 *f*).

The attractive side chain lysine$^+$ has an acceptor orbital which is localized on N^{ζ} but is otherwise much like that of alanine (Fig. 4 *a*). The histidine$^+$ orbital is similar to that of neutral histidine but with less density on the ring nitrogens and more density on $C^{\epsilon 1}$ (Fig. 4 *b*). The arginine acceptor orbital is of π^* symmetry and extends across the surface of the guanido group.

The acceptor level groupings can be rationalized using the language of molecular orbital theory. The semiconducting side chains are those with acceptor orbitals of π^* symmetry, or those with 3d-nonbonding symmetry. The acceptor orbitals of the insulating side chains are all of σ^* symmetry, and are strongly antibonding, thus they are expected to lie higher in energy than the semiconducting group. The semiconducting and insulating groups are bracketed from above and below by the repulsive and attractive side chains respectively. The acceptor levels for these groups can be explained in terms of coulombic interactions between the charged side chain and the extra electron.

As can be seen from Figs. 2–4, the energy ranking is also reflected in the extent of delocalization of the acceptor orbital; the acceptor orbitals of the semiconducting side chains are more highly delocalized than are those of the insulating group. It would be interesting to consider how this diffuseness relates to the extent of interaction between groups along a pathway.

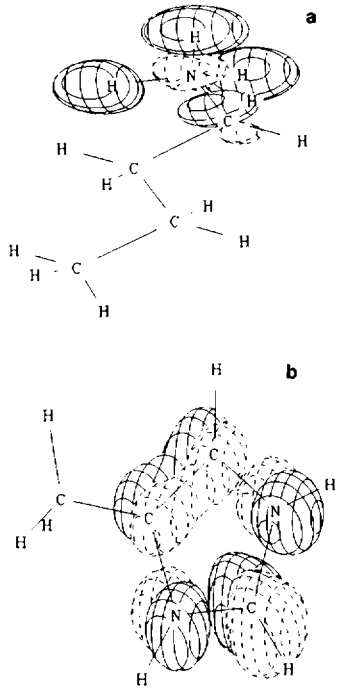

FIGURE 4 Acceptor orbitals for the attractive side chains. (*a*) Lysine orbital, like the alanine orbital localized on the terminal nitrogen. (*b*) The histidine acceptor orbital.

DISCUSSION

Marcus theory has been quite successful in describing electron transfer processes in solution. In this theory the medium between donor and acceptor is treated in an averaged way through free energy terms that account for the energy required to bring the donor and acceptor electronic energy levels into coincidence. At the point when solvent (medium) fluctuations have made the donor and acceptor electronic energies equal (or nearly so), we have the tunneling problem shown in Fig. 5.

The rate of tunneling may be modeled as though it were through a square potential barrier, which decays as $\exp(-\beta r)$, where β is the square root of the difference in vertical ionization potential between donor and medium (Fig. 5 *a*). Thus, β provides a measure of the ability of the medium to permit the transfer (conduction of an electron from the donor to the acceptor). This simple picture may be extended to potentials of arbitrary shape, as illustrated in Fig. 5 *b*. For tunneling through an arbitrarily shaped potential, the rate will decay as

$$\exp\left\{-C\int_{-a}^{a}[V(r)-E]^{1/2}\,dr\right\}, \qquad (4)$$

where $V(r)$ is a function that describes the potential energy of the barrier (from $-a$ to a in Fig. 5 *b*) (20–22) and C is a constant involving the mass of the electron and Planck's constant such that the argument of the exponent is dimensionless. We can see from Eq. 4 that the rate depends on the area under the potential barrier. In Marcus theory it is common to assume that the transmission rate decays as

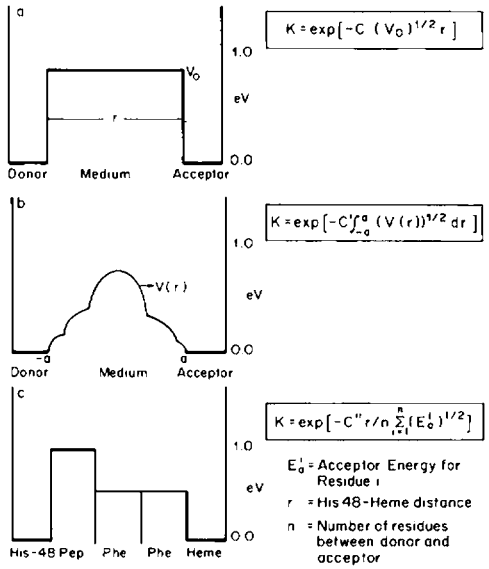

FIGURE 5 Transmission rate decay for various types of potential barrier. The dependence of the rate on the area beneath the barrier is illustrated for (*a*) a square potential barrier; (*b*) an arbitrary potential barrier described by the function $V(r)$. (*c*) A schematic representation of the His48–Heme barrier in myoglobin constructed from acceptor levels of the intervening side chains.

$\exp(-\beta r)$. Thus, tunneling through a potential of arbitrary shape can be thought of as tunneling through a square potential of height β^2, or as tunneling through a function $V(r)$ whose average height is β^2.

In the study of electron transfer in proteins, one can use the acceptor levels calculated here to estimate the area under the potential barrier for a given arrangement of amino acids separating the donor and acceptor. We have done this for the electron transfer between the heme group and the four ruthenium-modified histidines recently studied in myoglobin (11). Using computer graphics, we have determined those residues between the heme group and each of the four histidines, and constructed potential barriers similar to that depicted for the His48 pathway in Fig. 5 *c*. The height of each "square barrier" is the acceptor level for that residue, relative to an arbitrary zero set at the ionization limit. The width of each is made equal to the average distance per residue along the pathway, i.e., the transfer distance divided by the number of intervening residues. The acceptor orbitals of the aromatic side chains certainly span greater distances than the σ^* acceptor orbitals of the insulating side chains, however, we have set all residues to have equal width because, at this level of theory, a more detailed description of residue size or orientation would be inappropriate. Further, assigning residue widths from the crystal structure may be misleading because fluctuations are presumably required to attain the nuclear configuration of the transition point.

The area under the barrier computed from this description is simply

$$\frac{r}{n}\sum (\epsilon_a^i)^{1/2} = r(\beta[\epsilon_a]), \tag{5}$$

where r is the tunneling distance, n is the number of residues between donor and acceptor, and ϵ_a^i is the acceptor level of the ith residue. The electronic coupling parameter β is written as a function of ϵ_a to emphasize its dependence on the nature of the intervening residues. Proceeding in this way we obtained the following uncorrected β values for each pathway: $\beta_{his12} = 0.60$ Å^{-1}, $\beta_{his48} = 0.35$ Å^{-1}, $\beta_{his81} = 0.74$ Å^{-1}, and $\beta_{his116} = 0.77$ Å^{-1} (see Table I). The values for β have been calculated relative to a donor and acceptor electronic energy level of zero. The assumption that the donor and acceptor are at the zero of energy when the transfer takes place is arbitrary, therefore the values of β given here are relative, and may be shifted up or down upon detailed consideration of the donor-acceptor system. We note, however, it is the relative values of β that correlate the relative rates of transfer for iso-free energy processes.

The value of β is determined experimentally by taking the slope of a log-linear plot of rate versus distance. The points on this plot are taken from transfer rates in various proteins, where the donor-acceptor distance is inferred from the crystal structure. By drawing a line through these points one determines the single best-fit value for β. There are few proteins where both transfer rate and distance are known, so there are only a few points from which to infer a value of β. However, β values of between 0.7 Å^{-1} and 1.4 Å^{-1} have been reported for proteins (11); the value of β inferred from solution studies (10) is usually between 1.0 Å^{-1} and 2.0 Å^{-1}.

TABLE I
CHARACTERIZATION OF THE POTENTIAL BARRIER IN FOUR ELECTRON TRANSFER PATHWAYS IN MYOGLOBIN*

Pathway	Transfer distance	Intervening residues‡§	Area beneath barrier¶	Average barrier height¶	Coupling constant (β)¶
	Å		$eV^{1/2}$ Å	$eV^{1/2}$	Å^{-1}
His12	22.3	Pep. Val pep. Trp pep. (S, I, S, S, S)	26.2	1.17	0.60
His48	13.4	Pep. Phe Phe (S, S, S)	9.29	0.69	0.35
His81	18.2	Pep. pep. His Ile Phe Leu (S, S, S, I, S, I)	26.2	1.44	0.74
His119	19.6	Pep. pep. pep. Ile pep. Ile (S, S, S, I, S, I)	29.7	1.51	0.77

*Separation distances were taken from the x-ray crystal structure; intervening residues were determined by computer graphics.
‡pep., peptide amide group.
§S, semiconducting residue. I, insulating residue.
¶The area beneath the potential barrier, average barrier height, and coupling constant are uncorrected values, i.e., they are relative to a donor-acceptor electronic energy level set at the ionization limit.

To permit the correlation of calculated β values with those from the experiment, we have applied a constant shift of -1.35 eV to the donor-acceptor energy such that our lowest barrier pathway (His48) occurs at the lower limit of the range of β values found in proteins (0.7 Å^{-1}) (11). When we set the His48 pathway to 0.7 Å^{-1}, we obtain the following corrected values for β for the other three pathways: $\beta_{his12} = 0.88$ Å^{-1}, $\beta_{his81} = 0.98$ Å^{-1}, $\beta_{his116} = 1.00$ Å^{-1}. These corrected values suggest that β can vary significantly within a single protein, depending on which types of residues, and how many, lie between the donor and acceptor (Table I). In the His48 pathway ($\beta = 0.70$ Å^{-1}) for example, the medium is made up of a peptide group, and two phenylalanine side chains. As all of these are classified as semiconducting, we predict strong electronic coupling along this pathway. We obtain a value 0.88 Å^{-1} for the His12 pathway which consists of three peptide groups, a valine side chain, and a tryptophan side chain. The presence of an insulating residue in this pathway increases the value of β and leads us to predict only modest coupling here. Our largest value of β (1.00 Å^{-1}) occurs in the His116 pathway which contains two insulating and four semiconducting groups; we therefore predict weak coupling for this pathway. A pathway consisting entirely of semiconducting side chains (a single disulfide group for

example) could have a β as small as 0.60 $Å^{-1}$ within this model, while one with only insulating side chains (a single alanine for example) could have a β as large as 1.5 $Å^{-1}$. This range of β is consistent with that found for proteins. Water has an acceptor level of 7.4 eV, leading to a β value of 1.5 $Å^{-1}$ when calculated as above. This value falls within the range of β for solution studies given in reference 10, and is identical to that determined from studies in frozen media (23). Some care is necessary in interpreting the results of solution studies, however, as these often involve bridging groups between donor and acceptor, whence through-bond electron transfer may contribute to the rate. We await further experimental characterization of these pathways for full verification of the trends predicted here.

Several important approximations were made in this study and it is worthwhile to reiterate them at this point. First, we have used the INDO approximation to determine molecular orbitals, and Koopmans' theorem to justify equating the eigenvalue of an orbital with vertical ionization potentials. Both of these quantum chemical methods may be brought into question. However, even at a higher level of theory the outstanding qualitative features we observe are not expected to change dramatically, e.g., the side chain group delineations are expected to remain unaltered and the relative energy differences between each group should not change significantly. Second, the potential barrier was constructed as a sequence of square wells, where there is no accounting for orientation of, or interaction between, adjacent groups. We also have not accounted for local electric fields, which may be large, e.g., due to a nearby helix dipole. We are currently calculating the effect of oriented electric fields on the acceptor level of each side chain. In future work we will be calculating the electronic coupling between adjacent groups to determine how the acceptor level of a side chain is affected by its neighbors.

CONCLUSION

We have devised a new classification of the amino acid side chains based on the doublet acceptor energy level. The side chains fall into four groups in this classification, suggesting that some side chains propagate electronic coupling more effectively than do others. Using the acceptor levels as a measure of this propensity, we are able to estimate the electronic coupling along a proposed electron transfer pathway by constructing a potential barrier and determining the area beneath it. The rate of electron transfer decays as the exponential of this area. We have applied this approach to determine the coupling constant β for each of four pathways in myoglobin, and have found that β varies from 0.70 $Å^{-1}$ to 1.00 $Å^{-1}$, which is consistent with values inferred for proteins (10, 11). This result emphasizes that β is a function of the residues which are between the donor and acceptor, and does not have a single value in proteins.

We anticipate the classification scheme put forth in the present paper will provide a natural language for describing medium effects on electron transfer rates in proteins. Quantitative predictions from the present level of theory cannot, however, be made; in future research the role of orientation and fluctuations will be considered. Predictions can be made concerning the relative electronic couplings, and our findings indicate that these should vary substantially for the four pathways in rutheniated-myoglobin; values ranging from 0.7 $Å^{-1}$ to 1.00 $Å^{-1}$ are found. To fully test these predictions one would need to evaluate rates for pathways that differed only by single amino acid substitutions, since $\beta(\epsilon_a)$ is a function of the individual residues between the donor and acceptor. Such site directed mutagenesis is currently being carried out by several research groups (11, 24) and we anticipate that the forthcoming experimental results will provide additional information to be used in refining current models.

We would like to acknowledge Professor Robert Birge and Leonore Findsen for helpful discussions of the ZINDO methods.

S. F. Sneddon would like to acknowledge support from the Office of Naval Research graduate fellowship program. Support for this work from the National Institutes of Health, grant GM37554-01, is also acknowledged.

Received for publication 10 August 1987 and in final form 22 September 1987.

REFERENCES

1. Creighton, T. E. 1984. Proteins. W. H. Freeman and Co., New York.
2. Chou, P. Y., and G. D. Fasman. 1987. Prediction of the secondary structure of proteins from their amino acid sequence. *Adv. Enzymol.* 47:45–148.
3. Eisenberg, D., W. Wilcox, and S. M. Eshita. 1986. Free energy and protein folding: Hydrophobic moments and solvation free energy. *In* Computer Graphics. Chapter 11. Cold Spring Harbor Laboratory, Cold Spring Harbor, NY.
4. Baldwin, R. L. 1986. Temperature dependence of the hydrophobic interaction in protein folding. *Proc. Natl. Acad. Sci. USA.* 83:8069.
5. Kauzmann, W. 1987. Thermodynamics of unfolding. *Nature (Lond.).* 325:763.
6. Shindo, H., and J. S. Cohen. 1976. Nuclear magnetic resonance titration curves of histidine ring protons. *J. Biol. Chem.* 251:2648.
7. Matthew, J. B., and F. M. Richards. 1982. Anion binding and pH-dependant electrostatic effects in ribonuclease. *Biochemistry.* 21:4989.
8. Pople, J. A., and D. L. Beveridge. 1970. Approximate Molecular Orbital Theory. McGraw-Hill Book Co., New York.
9. Pople, J. A., D. L. Beveridge, and P. A. Dobosh. 1967. Approximate self-consistent molecular-orbital theory. V. Intermediate neglect of differential overlap. *J. Chem. Phys.* 47:2026–2033.
10. Marcus, R. A., and N. Sutin. 1985. Electron transfers in chemistry and biology. *Biochim. Biophys. Acta.* 811:265–322.
11. Mayo, S. L., W. R. Ellis, R. J. Crutchley, and H. B. Gray. 1986. Longe-range electron transfer in heme proteins. *Science (Wash. DC.).* 233:948–952.
12. Bacon, A. D., and M. C. Zerner. 1979. An intermediate neglect of differential overlap theory for transition metal complexes: Fe, Co, and Cu^+ chlorides. *Theor. Chim. Acta. (Berl.)* 53:21.
13. Koopmans, T. 1933. The distribution of wave function and characteristic value among the individual electrons of an atom. *Physica.* 1. 104.
14. Takano, T. 1977. *J. Mol. Biol.* 110:569. (Coordinates were taken from the Brookhaven Protein Data Bank.)

15. Fuita, H., and A. Imamura. 1970. Electronic structures of polymers using the tight-binding approximation. II. Polyethylene and polyglycine by the CNDO method. *J. Chem. Phys.* 53:4555.
16. Duke, B. J., J. E. Eilers, and B. O'Leary. 1975. The simulated ab-initio molecular orbital method for polymers: polyglycine. *Chem. Phys. Lett.* 32:602.
17. Deleted in press.
18. PSI/77, W. L. Jorgensen, Program No. 340. Quantum Chemistry Program Exchange, Indiana University, Bloomington, IN.
19. Tedder, J. M., and A. Nechvatal. 1985. Pictorial Orbital Theory. Pitman Publishing Inc., London.
20. Bell, R. P. 1980. The Tunnel Effect in Chemistry. Chapman and Hall, New York.
21. Petrov, F. G. 1979. Mechanisms of electron transfer through proteins. *Int. J. Quantum Chem. Symp.* 16:133–152.
22. De La Vega, J. R. 1982. Role of symmetry in the tunnelling of the electron in double minimum potentials. *Acc. Chem. Res.* 15:185–191.
23. Alexandrov, I. V., R. F. Khairutdinov, and K. I. Zamarev. 1978. Electron tunneling in solid phase redox reactions. Experimental values of parameters characterizing the rate of tunneling and theoretical models for long range electron transfer. *Chem. Phys. Lett.* 32:123–141.
24. Isied, S. S., C. Kuehn, and G. Worosila.1984. Ruthenium-modified cytochrome *c*: temperature dependence of the rate of intramolecular electron transfer. *J. Am. Chem. Soc.* 106:1722–1726.